Setd2 regulates quiescence and differentiation of adult hematopoietic stem cells by restricting RNA polymerase II elongation

Yile Zhou,[1,2] Xiaomei Yan,[2] Xiaomin Feng,[2] Jiachen Bu,[2,3] Yunzhu Dong,[2] Peipei Lin,[2] Yoshihiro Hayashi,[2] Rui Huang,[2] Andre Olsson,[4] Paul R. Andreassen,[2] H. Leighton Grimes,[4] Qian-fei Wang,[3] Tao Cheng,[5] Zhijian Xiao,[5] Jie Jin[1,*] and Gang Huang[2,*]

[1]Department of Hematology, The First Affiliated Hospital, Zhejiang University School of Medicine, Hangzhou, China; [2]Division of Pathology and Experimental Hematology and Cancer Biology, Cincinnati Children's Hospital Medical Center, OH, USA; [3]Laboratory of Genome Variations and Precision Bio-Medicine, Beijing Institute of Genomics, Chinese Academy of Sciences, China; [4]Division of Immunobiology and Center for Systems Immunology, Cincinnati Children's Hospital Medical Center, OH, USA; and [5]State Key Laboratory of Experimental Hematology, Institute of Hematology and Blood Diseases Hospital and Center for Stem Cell Medicine, Chinese Academy of Medical Sciences and Peking Union Medical College, Tianjin, China

**JJ and GH contributed equally to this study as joint senior authors*

Haematologica 2018
Volume 103(7):1110-1123

ABSTRACT

SET domain containing 2 (*Setd2*), encoding a histone methyltransferase, is associated with many hematopoietic diseases when mutated. By generating a novel exon 6 conditional knockout mouse model, we describe an essential role of *Setd2* in maintaining the adult hematopoietic stem cells. Loss of *Setd2* results in leukopenia, anemia, and increased platelets accompanied by hypocellularity, erythroid dysplasia, and mild fibrosis in bone marrow. *Setd2* knockout mice show significantly decreased hematopoietic stem and progenitor cells except for erythroid progenitors. *Setd2* knockout hematopoietic stem cells fail to establish long-term bone marrow reconstitution after transplantation because of the loss of quiescence, increased apoptosis, and reduced multiple-lineage terminal differentiation potential. Bioinformatic analysis revealed that the hematopoietic stem cells exit from quiescence and commit to differentiation, which lead to hematopoietic stem cell exhaustion. Mechanistically, we attribute an important *Setd2* function in murine adult hematopoietic stem cells to the inhibition of the Nsd1/2/3 transcriptional complex, which recruits super elongation complex and controls RNA polymerase II elongation on a subset of target genes, including *Myc*. Our results reveal a critical role of *Setd2* in regulating quiescence and differentiation of hematopoietic stem cells through restricting the NSDs/SEC mediated RNA polymerase II elongation.

Introduction

Hematopoietic stem cells (HSCs) are characterized by their capability for self-renewal and multi-potency.[1,2] Hematopoiesis is dynamically controlled by the interplay of transcriptional and epigenetic networks, while dysregulation of these networks can lead to unfitness of hematopoiesis, cellular transformation, and hematologic diseases. Multiple drugs targeting epigenetic modulators have shown promising effects on certain hematopoietic diseases.[3,4] Thus, a better understanding of how the epigenome is regulated in hematopoiesis may provide insights that can improve the treatment of hematologic disorders.

Correspondence:

gang.huang@cchmc.org or
jiej0503@zju.edu.cn

Received: Juanary 3, 2018.
Accepted: April 6, 2018.
Pre-published: April 12, 2018.

doi:10.3324/haematol.2018.187708

Check the online version for the most updated information on this article, online supplements, and information on authorship & disclosures: www.haematologica.org/content/103/7/1110

Histone H3K36 methylation is one of the most prominent epigenetic modifications that are associated with gene activation. In yeast, Set2 is the sole H3K36 methyltransferase, which is responsible for all three methylation events and can interact with RNA polymerase II (RNA Pol II).[5] Set2 contains several conserved domains. One of them is the SET domain, which is the catalytic domain for H3K36 methylations. Another important domain is the SRI domain, which binds to serine 2 (Ser2) and serine 5 (Ser5) doubly phosphorylated carboxyl terminal domain (CTD) repeats of RNA Pol II.[6] The human ortholog of Set2, SETD2, was first isolated from human $CD34^+$ hematopoietic stem/progenitor cells (HSPCs).[7] SETD2 mainly works as H3K36 tri-methyltransferase, while H3K36me1 and H3K36me2 are catalyzed by other methyltransferases. To date, 7 other HMT enzymes have been reported to methylate H3K36, including NSD1, NSD2, NSD3, and ASH1L.[8] NSD1/2/3 and ASH1L can methylate H3K36 to generate H3K36me1 and H3K36me2. The NSDs have been reported as oncogenic drivers in many cancers including leukemia. Furthermore, NSDs could regulate WNT, MYC, and NF-κB to affect various physiological or pathological processes.[9]

It has been reported that *Setd2* is required for murine embryonic stem cells (mESCs) differentiation toward endoderms and endoderm development during murine embryonic development,[10] while *Setd2*$^{-/-}$ resulted in embryonic lethality at E10.5-11.5.[11] *SETD2* was identified as a tumor suppressor, as loss-of-function (LOF) mutations of *SETD2* have been found in many human cancers, including leukemia and lymphoma.[12-15] Previously, we have reported that there are *SETD2* mutations in 6% of acute leukemia with 22% enriched in *MLL*-rearranged leukemia.[16] However, the roles of *SETD2* in adult HSPCs and normal hematopoiesis have not been fully studied. To understand the mechanisms of how *Setd2* regulates the normal hematopoiesis, by using a novel conditional knockout model, we revealed a unique and critical role of *Setd2* in regulating quiescence and differentiation of adult HSCs through restricting NSDs/SEC mediated RNA polymerase II elongation.

Methods

Animals

Setd2$^{f/f}$ (B6, CD45.2) mice were generated by Cincinnati Children's Hospital Transgenic Core. *Vav1-Cre*, *Mx1-Cre*, *Tie2-Cre* mice were purchased from Jackson Laboratory. All mice were housed in the rodent barrier facility at Cincinnati Children's Hospital Medical Center (CCHMC).

Small molecular inhibitors treatment

The CD117 positive selection of bone marrow (BM) cells was performed using magnetic CD117 microbeads (Miltenyi 130-091-224) following the manufacturer's instructions. The CD117 positive fractions were cultured in medium (Stemspan+100 ng/mL SCF+100 ng/mL TPO) and treated with JQ1 500 nM, EPZ-5676 1uM, BAY 1143572 400 nM for 24 and 48 hours (h). The inhibitors were from the following companies: JQ1 (Sigma-Aldrich, SML0974), EPZ-5676 (Selleckchem, S7062), BAY 1143572 (MedChem Express, HY-12871).

Details of the methods used are available in the *Online Supplementary Appendix*.

Results

Generating a novel *Setd2* conditional knockout allele

Setd2 is involved in the ESCs differentiation and vascular formation during embryonic development. *Setd2*$^{-/-}$ mice are embryonic lethal.[10] Thus, we generated a *Setd2* conditional knockout allele by inserting two LoxP sites flanking *Setd2* exon6, which encodes part of the SET domain. Deletion of exon 6 could result in frame-shift and trigger nonsense-mediated decay (NMD) of the mutant mRNA transcript (*Online Supplementary Figure S1A*). Three Cre transgenic lines were used: *Tie2-Cre*, *Mx1-Cre*, and *Vav1-Cre*. *Tie2-Cre* mice display Cre activities in both endothelial cells and hematopoietic cells.[17] However, we were unable to develop any *Setd2*$^{f/f}$*/Tie2-Cre* mice by intercrossing *Setd2*$^{f/w}$*/Tie2-Cre* mice with *Setd2*$^{f/f}$ mice in multiple litters (*Online Supplementary Table S1*), while polyinosinic-polycytidylic acid (pIpC) induced *Setd2*$^{f/f}$*/Mx1-Cre* mice and *Setd2*$^{f/f}$*/Vav1-Cre* mice are viable and fertile. Thus, we focused on Mx1-Cre and Vav1-Cre alleles to achieve *Setd2*$^{f/f}$ deletion in the hematopoietic system.

First, to confirm *Setd2* deletion, the mice were genotyped using tail tissue and peripheral blood by genomic PCR (*Online Supplementary Figure S1B and C*). The LoxP insertion and *Setd2* deletion were confirmed in *Setd2*$^{f/f}$ and *Setd2*$^{f/f}$*/Vav1-Cre* mice. Subsequently, the *Setd2* expressions were confirmed to be dramatically decreased at both mRNA and protein levels in *Setd2*$^{f/f}$*/Vav1-Cre* mice and pIpC induced *Setd2*$^{f/f}$*/Mx1-Cre* mice BM cells (Figure 1A, *Online Supplementary Figure S1D*, and *data not shown*). Consistent with the role of *Setd2* in regulating H3K36 methylation, global H3K36me3 was significantly reduced in BM cells of *Setd2* knockout mice (Figure 1A).

Setd2$^{\Delta/\Delta}$ mice showed leukopenia, anemia, erythroid dysplasia, increased thrombopoiesis, and mild BM fibrosis

Setd2$^{f/f}$*/Vav1-Cre* mice are born small and pale. When the circulating blood count (CBC) was checked at eight weeks, they showed leukopenia, macrocytic anemia, and increased platelet count compared to the control littermates (Figure 1B-D). To exclude the possibility that the phenotype is contingent on deletion early in fetal hematopoiesis, we induced excision in 6- to 10-week old *Setd2*$^{f/f}$*/Mx1-Cre* mice with pIpC injection. We found similar phenotypes two weeks after pIpC injection (*Online Supplementary Figure S2A-C*).

Consistent with peripheral blood (PB) phenotype, the *Setd2*$^{\Delta/\Delta}$ mice, both *Setd2*$^{f/f}$*/Vav1-Cre* and *Setd2*$^{f/f}$*/Mx1-Cre* models, had 30% fewer nucleated BM cells, enlarged spleens, and obviously shrunken thymuses (Figure 1E-G and *Online Supplementary Figure S2D*), which were also confirmed by pathology. There are significantly increased erythroblasts and mature megakaryocytes in *Setd2*$^{\Delta/\Delta}$ mice BM compared to the controls (*Online Supplementary Table S2*). Notably, the percentage of erythroblasts gradually increases with aging and could even reach up to 80% in some mice (*data not shown*). Erythroid dysplasia could also be observed. Compared with the round nuclei of erythroblasts in control mice, erythroblasts in *Setd2*$^{\Delta/\Delta}$ mice showed frequent multi-nucleation, nuclear budding, nuclear fragments, and more cells in mitosis (Figure 1H). However, no obvious dysplasia was observed in other myeloid lineages or megakaryocytes. In addition to erythroid dysplasia, the histology showed increased reticulin

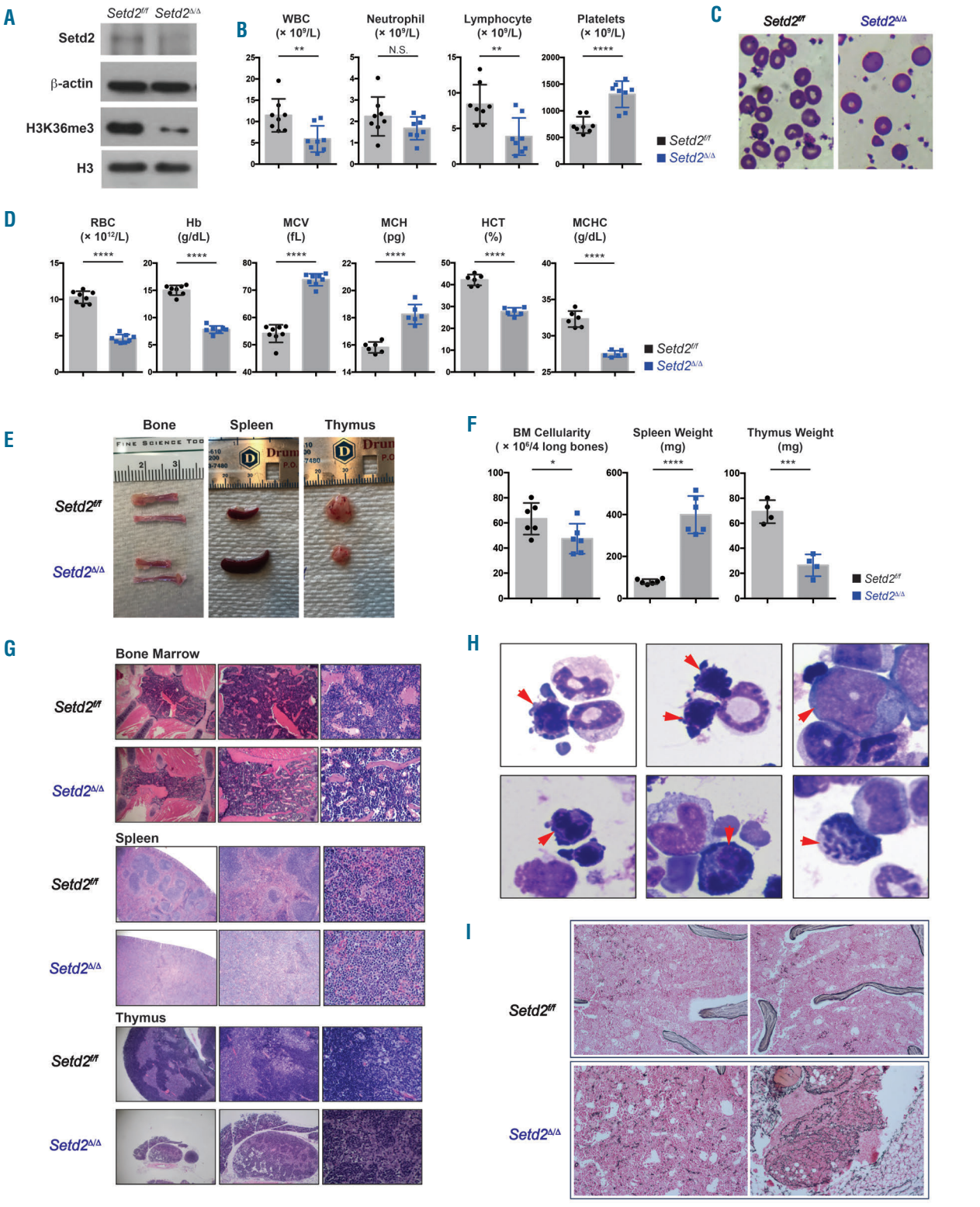

Figure 1. *Setd2*$^{\Delta/\Delta}$ mice showed leukopenia, anemia, erythroid dysplasia, increased thrombopoesis and mild bone marrow (BM) fibrosis. (A) Setd2 and H3K36me3 protein levels were determined by immunoblotting using c-Kit$^+$ BM cells. Representative data were from 3 independent experiments. [N=3; mean±Standard Deviation (SD)]. (B) Complete blood count of *Setd2*$^{f/f}$*/Vav1-Cre* mice, showing reduced white blood cells, lymphocytes, neutrophils, and platelets. [N=8 mice per genotype; mean±Standard Error of Mean (SEM)]. (C) Representative photos of Wright's stained peripheral blood smear of *Setd2*$^{f/f}$ and *Setd2*$^{f/f}$*/Vav1-Cre* mice. (D) Complete blood count of *Setd2*$^{f/f}$*/Vav1-Cre* mice, showing reduced red blood cells, hemoglobin content, red blood cell specific volume (HCT), mean corpuscular hemoglobin concentration (MCHC), but increased mean corpuscular volume of red cells (MCV) and mean corpuscular hemoglobin (MCH). (N=8 mice per genotype; mean±SEM). (E) Representative photos of bones (tibia and fibula), spleens, and thymuses in *Setd2*$^{f/f}$ and *Setd2*$^{f/f}$*/Vav1-Cre* mice. (F) BM cellularity, spleen weight, and thymus weight of *Setd2*$^{f/f}$ and *Setd2*$^{f/f}$*/Vav1-Cre* mice. (N≥4 mice per genotype; mean±SEM). (G) Representative photos of hematoxylin & eosin-stained sections from the sternum, spleens, thymuses of *Setd2*$^{f/f}$ and *Setd2*$^{f/f}$*/Vav1-Cre* mice. (H) Dysplastic erythroid cells can be found in BM cytospin: megaloblastic erythroid precursors, dysplatic erythroid precursors with multi-nucleation, nuclear fragments, or nuclear budding. In addition, erythroid cells can be caught in mitosis. (I). Representative photos of reticulin-stained sections from sternum of *Setd2*$^{f/f}$ and *Setd2*$^{f/f}$*/Vav1-Cre* mice.

staining in *Setd2*$^{\Delta/\Delta}$ mice BM (Figure 1I). Compared with some scattered punctual and linear reticulin in the control, scattered linear reticulin with loose network and some focal density increases in reticulin could be found in *Setd2*$^{\Delta/\Delta}$ BM within four months, which could be classified into mild BM fibrosis (grade 1 or 2).[18]

Setd2$^{\Delta/\Delta}$ mice showed profound reduction of myeloid, lymphoid, and megakaryocytic progenitors, but significantly increased erythroid progenitors

To understand leukopenia and anemia in *Setd2*$^{\Delta/\Delta}$ mice, we first examined the BM progenitor populations by flow cytometry. Significant reductions in the absolute number of CLP, Pre-GM, GMP, Pre-MegE, and MkP were found, while the absolute number of Pre CFU-E was dramatically increased (Figure 2A and B).

It is noteworthy that *Setd2*$^{\Delta/\Delta}$ mice showed anemia in PB but significantly increased Pre CFU-Es in BM. To understand the remarkable differences between these two phenotypes, a detailed analysis of erythroid differentiation was performed. There were increased proportions of nucleated erythroblasts accompanied by a decreased proportion of enucleated erythrocytes in *Setd2*$^{\Delta/\Delta}$ mice (*Online Supplementary Figure S3A and B*), indicating the defective terminal erythroid differentiation. Meanwhile, a reduction of MkPs in BM, accompanied by an increase in platelet counts in PB, was observed in *Setd2*$^{\Delta/\Delta}$ mice. In the analysis of polyploidy using BM CD41$^+$ cells, the *Setd2*$^{\Delta/\Delta}$ mice displayed significantly increased distributions of hyper-polyploidy (16N and 32N) cells and reduced distributions of low- to intermediate-ploidy (2N-8N) cells (*Online Supplementary Figure S3C* and *D*). In addition, more megakaryocytes were observed in both BM cytospins and spleen histology slides in *Setd2*$^{\Delta/\Delta}$ mice compared with control (*Online Supplementary Table S2* and *Online Supplementary Figure S3E*).

To determine HPC functional activity besides phenotypic changes, we performed colony-forming unit (CFU) assays, which showed that almost all types of colony numbers were decreased except the burst-forming unit-erythroid (BFU-E). Interestingly, the BFU-E could even be detected in the 4th replating, while all other colonies stopped growing after three incidences of replating in the controls (Figure 2C). To further confirm the erythroid-related results, the CFU-E assays were performed in M3334 medium, which contains erythropoietin (EPO) only. After 48 h, *Setd2*$^{\Delta/\Delta}$ BM cells showed significantly increased BFU-E/CFU-E colony frequencies and the colonies were larger in size compared with colonies from the controls (Figure 2D). These results indicate that *Setd2* is critical in maintaining normal HPC numbers and lineage specification.

Depletion of phenotypic and functional HSCs in *Setd2*$^{\Delta/\Delta}$ mice

Next, we examined the bone marrow HSC populations. Significant reductions, in absolute number and frequency, of LSKs, SLAM-HSCs, and MPPs were found in *Setd2*$^{\Delta/\Delta}$ mice compared with the controls (Figure 3A and B).

To determine the HSC activity, a series of bone marrow transplantation (BMT) assays were performed. We first evaluated the HSC function in a competitive bone marrow transplantation assay (CBMT). Lethally irradiated CD45.1$^+$ recipient mice were transplanted using an equal number of BM cells from both CD45.1$^+$ competitors and CD45.2$^+$ *Setd2*$^{f/f}$ or *Setd2*$^{f/f}$*/Mx1-Cre*. Sixteen weeks after CBMT, *Setd2*$^{\Delta/\Delta}$ cells were outcompeted to less than 1% in PB (Figure 3C). In the BM, *Setd2*$^{\Delta/\Delta}$ failed to support long-term reconstitution of the Gr1$^+$CD11b$^+$ population (myeloid), B220$^+$ population (B cells), and CD3$^+$ population (T cells). Analysis of BM LSKs showed a complete absence of *Setd2*$^{\Delta/\Delta}$ LSKs (Figure 3D). Similar results were observed by using *Setd2/Vav1-Cre* BM cells in CBMT assay (Figure 3E). To exclude the possibility that BM microenvironment defects (such as endothelial cells and stromal BM cells) may contribute to HSC dysfunction, we transplanted BM cells from *Setd2*$^{f/f}$ or *Setd2*$^{f/f}$*/Mx1-Cre* mice into lethally irradiated CD45.1$^+$ recipient mice. We found similar engraftment four weeks after transplantation, around 90% engraftment in both groups. Then we deleted *Setd2* in donor-derived grafts with pIpC injection. We found decreased donor-derived cell chimerism in *Setd2*$^{\Delta/\Delta}$ mice (Figure 3F). The PB phenotypes of BMT mice are similar to the primary knockout mice, which also manifested leukopenia, macrocytic anemia, and increased platelet counts (Figure 3G). However, when non-competitive transplantation with *Setd2*$^{f/f}$*/Vav1-Cre* BM cells were performed, all the recipients died within 75 days (Figure 3H). When complete PB count was checked at 28 days post BMT, recipient mice showed severe pancytopenia, indicating the failure of BM reconstitution (*Online Supplementary Figure S4A*). These results indicate that *Setd2*$^{\Delta/\Delta}$ HSCs have intrinsic defects in BM reconstitution.

Setd2$^{\Delta/\Delta}$ HSCs show reduced self-renewal and quiescence, but increased proliferation, apoptosis, and differentiation.

To identify the *Setd2*$^{\Delta/\Delta}$ HSC functions under chemotherapeutic stress, we next challenged *Setd2*$^{\Delta/\Delta}$ and control mice with 5-fluorouracil (5-FU). In the 8-day recovery group, a single 5-FU treatment resulted in a 10-fold reduction of BM cellularity and a 2-fold reduction of SLAM-HSCs in the control, but a 20-fold reduction of BM cellularity and a 5-fold reduction in *Setd2*$^{\Delta/\Delta}$ mice (Figure 4A). In the 5-FU weekly treated group, *Setd2*$^{\Delta/\Delta}$ mice could tolerate 2 cycles of 5-FU injections, while all the control mice could tolerate 3 cycles (Figure 4B). These results indicated that *Setd2*$^{\Delta/\Delta}$ mice were more sensitive to 5-FU. 5-FU kills dividing cells but spares quiescent cells, such as stem cells, and subsequently forces HSCs to proliferate to reconstitute the BM; thus *Setd2*$^{\Delta/\Delta}$ HSCs might have intrinsic defects in maintaining normal quiescence.

Next, the cell cycle status was assessed. *Setd2*$^{\Delta/\Delta}$ HSCs had a markedly reduced G0 fraction and increased entries into G1 and S/G2/M phases of the cell cycle (Figure 4C). *Setd2*$^{\Delta/\Delta}$ SLAM-HSCs also exhibited increased incorporation of BrdU into the DNA, indicative of more cycling cells (*Online Supplementary Figure S4B*). These results suggested that *Setd2*$^{\Delta/\Delta}$ HSCs could not maintain a normal quiescent state and subsequently enter the cell cycle. Also, apoptotic status was assessed in *Setd2*$^{\Delta/\Delta}$ and control mice. There were significantly increased proportions of Annexin V$^+$ SLAM-HSC, LSK, and LK cells, which demonstrated that *Setd2*$^{\Delta/\Delta}$ HSPCs underwent more cell death (Figure 4D and *Online Supplementary Figure S4C*).

To investigate the differentiation potential of *Setd2*$^{\Delta/\Delta}$ HSCs, single SLAM-HSCs were sorted and cultured in cytokine-containing medium. With this culture condi-

tion, 4 lineages could be observed, erythroid cells, megakaryocytes, neutrophils, and macrophages, in the single SLAM-HSC generated clones after 10-14 days. First, *Setd2*$^{\Delta/\Delta}$ SLAM-HSCs showed decreased clonogenicities, as there were significantly less HSCs that could generate clones in each plate in the *Setd2*$^{\Delta/\Delta}$ group compared with the control, while the sorting efficiency was comparable between these two groups (Figure 4E). In addition, *Setd2*$^{\Delta/\Delta}$ SLAM-HSCs produced fewer frequencies of 4-lineage clones compared with the control, accompanied

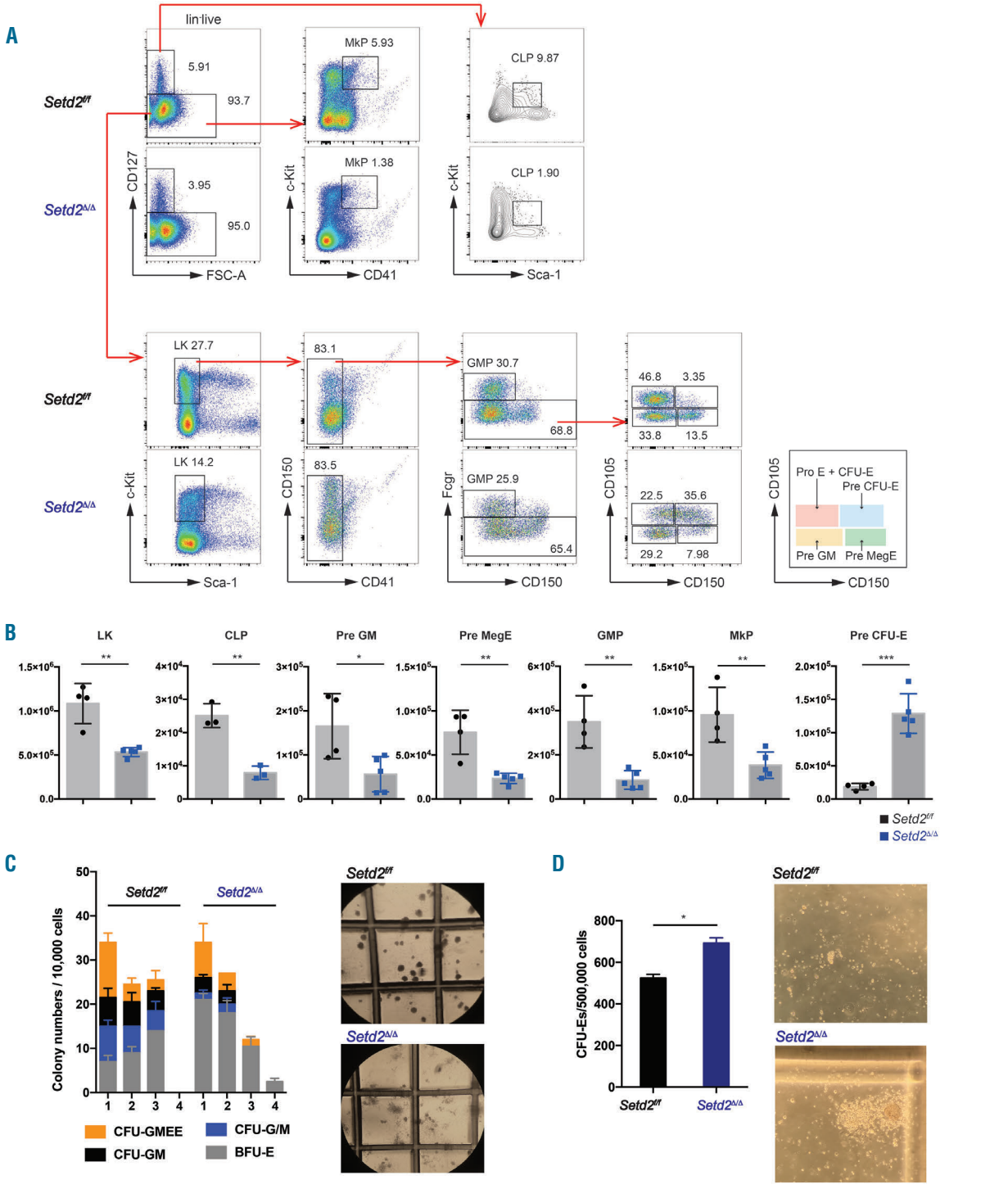

Figure 2. *Setd2*$^{\Delta/\Delta}$ mice showed profound reduction of myeloid, lymphoid and megakaryocyte progenitors but significantly increased erythroid progenitors. (A) Flow cytometry analysis of *Setd2*$^{f/f}$ and *Setd2*$^{f/f}$*/Vav1-Cre* mice bone marrow (BM) cells. (B) Absolute number of hematopoietic progenitor cell (HPC) populations. [*Setd2*$^{f/f}$ =4, *Setd2*$^{f/f}$*/Vav1-Cre*=5; mean±Standard Error of Mean (SEM)]. (C) Colony-forming cell (CFU) using BM cells from *Setd2*$^{f/f}$ or *Setd2*$^{f/f}$*/Vav1-Cre*. 2x10^4 cells were plated in M3434 in triplicate and colonies were scored every seven days. GEMM: granulocyte, erythroid, macrophage, megakaryocyte colony; GM: granulocyte/macrophage; G/M: granulocyte or macrophage; BFU-E: burst formation unit-erythroid. Representative data were from 3 independent experiments. (N=3; mean±Standard Deviation (SD)]. (D) CFU-erythroid (CFU-E) assay using BM cells from *Setd2*$^{f/f}$ or *Setd2*$^{f/f}$*/Vav1-Cre*. 5x10^5 cells were plated in M3334 in triplicate and colonies were scored 48 hours later. Representative data were from 3 independent experiments. (N=3; mean±SD).

with increased frequencies of 3-, 2-, and 1-lineage clones (Figure 4E). These results indicated that *Setd2*$^{\Delta/\Delta}$ SLAM-HSCs lost normal clonogenicity and multi-lineage differentiation potential, which indicated that *Setd2*$^{\Delta/\Delta}$ SLAM-HSCs were in a more differentiated state.

Setd2$^{\Delta/\Delta}$ HSPCs show a loss of stem cell identity and an increase in differentiation toward progenitors

There was a 4-fold reduction of SLAM-HSC numbers in *Setd2*$^{\Delta/\Delta}$ mice but a complete loss of HSC functions in the BMT assay. Thus, we consider it unlikely that the reduc-

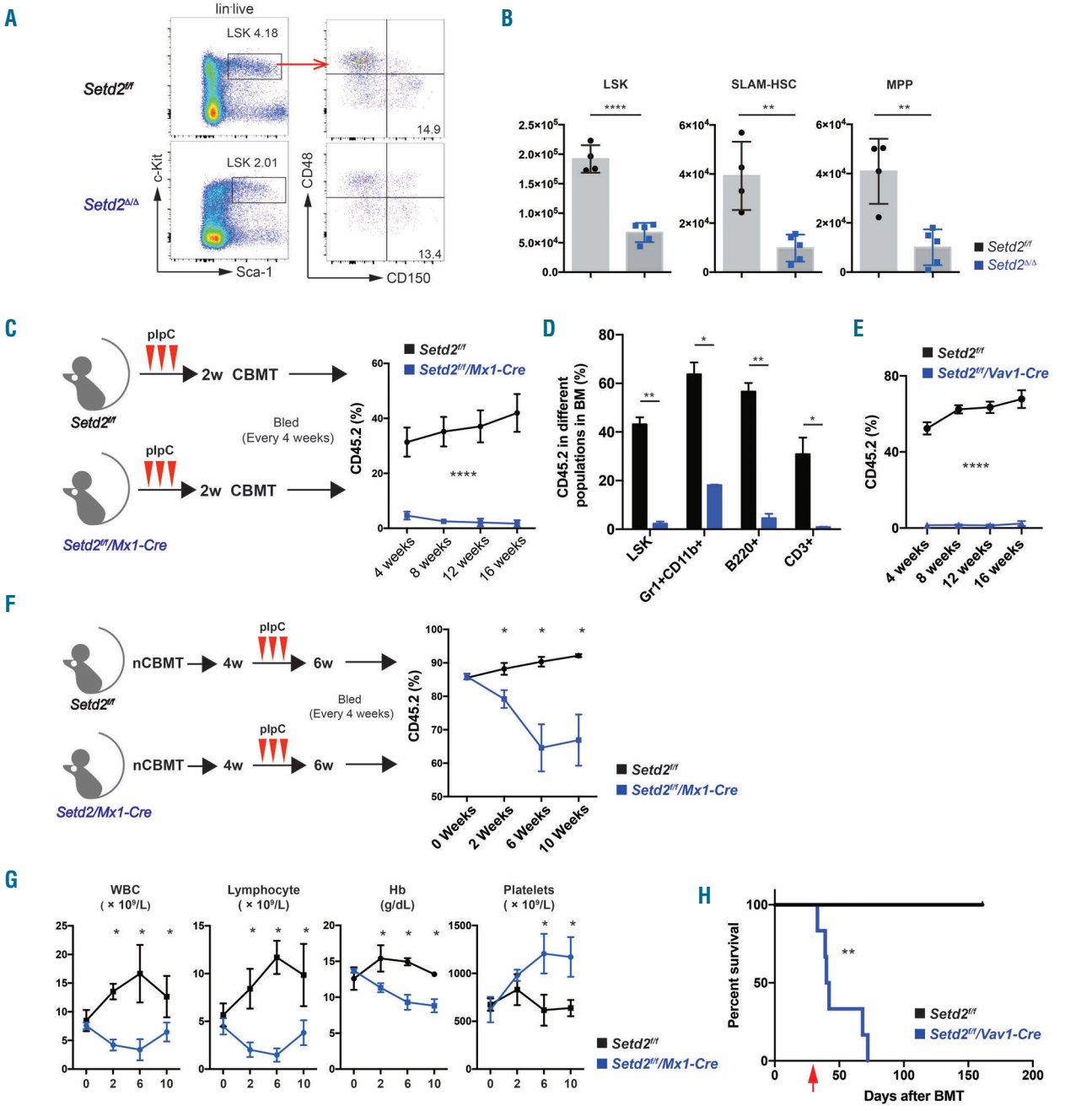

Figure 3. *Setd2*$^{\Delta/\Delta}$ mice had depletion of phenotypic and functional hematopoietic stem cells (HSCs). (A) Flow cytometry analysis of *Setd2*$^{f/f}$ and *Setd2*$^{f/f}$*/Vav1-Cre* mice bone marrow (BM) cells. (B) Absolute number of HSC populations. (*Setd2*$^{f/f}$ =4, *Setd2*$^{f/f}$*/Vav1-Cre*=5; mean±Standard Error of Mean (SEM)] (C). Experimental strategy: *Setd2*$^{f/f}$ or *Setd2*$^{f/f}$*/Mx1-Cre* (pIpC injected) CD45.2 BM cells (1.5×10^6 cells each) was injected into irradiated (7.5+4.25Gy) B6-CD45.1 recipients, with B6-CD45.1 competitor BM (1.5×10^6 cells each). Peripheral blood (PB) was analyzed 2-16 weeks after competitive transplantation. Representative data were from 2 independent experiments. (N=8 each genotype; mean±SEM). (D) CD45.1/CD45.2 chimerism in BM LSKs, Gr1$^+$CD11b$^+$ myeloid cells, B220$^+$ B cells, CD3$^+$ T cells 16 weeks after transplantation. Representative data were from 2 independent experiments. (N=8 each genotype; mean±SEM). (E) Experimental strategy: *Setd*$^{f/f}$ or *Setd2*$^{f/f}$*/Vav1-Cre* CD45.2 BM cells (1.5×10^6 cells each) was injected into irradiated (7.5+4.25Gy) B6-CD45.1 recipients, with B6-CD45.1 competitor BM (1.5×10^6 cells each). PB was analyzed 4-16 weeks after competitive transplantation. Representative data were from 2 independent experiments. (N=8 each genotype; mean±SEM). (F and G) Experimental strategy: *Setd2*$^{f/f}$ or *Setd2*$^{f/f}$*/Mx1-Cre* CD45.2 BM was injected into irradiated (7.5+4.25Gy) B6-CD45.1 recipients (2×10^6 cells per genotype), with B6-CD45.1 helper BM (1×10^5 cells). pIpC was injected two weeks after BMT. Peripheral blood were analyzed 0-10 weeks after pIpC injection. Representative data were from 2 independent experiments. (N=8 each genotype; mean±SEM). (H) Experimental strategy: *Setd2*$^{f/f}$ or *Setd2*$^{f/f}$*/Vav1-Cre* CD45.2 BM was injected into irradiated (7.5+4.25Gy) B6-CD45.1 recipients (2×10^6 cells per genotype), with B6-CD45.1 helper BM (1×10^5 cells), survival conditions were monitored. (N=6 each genotype; mean±SEM).

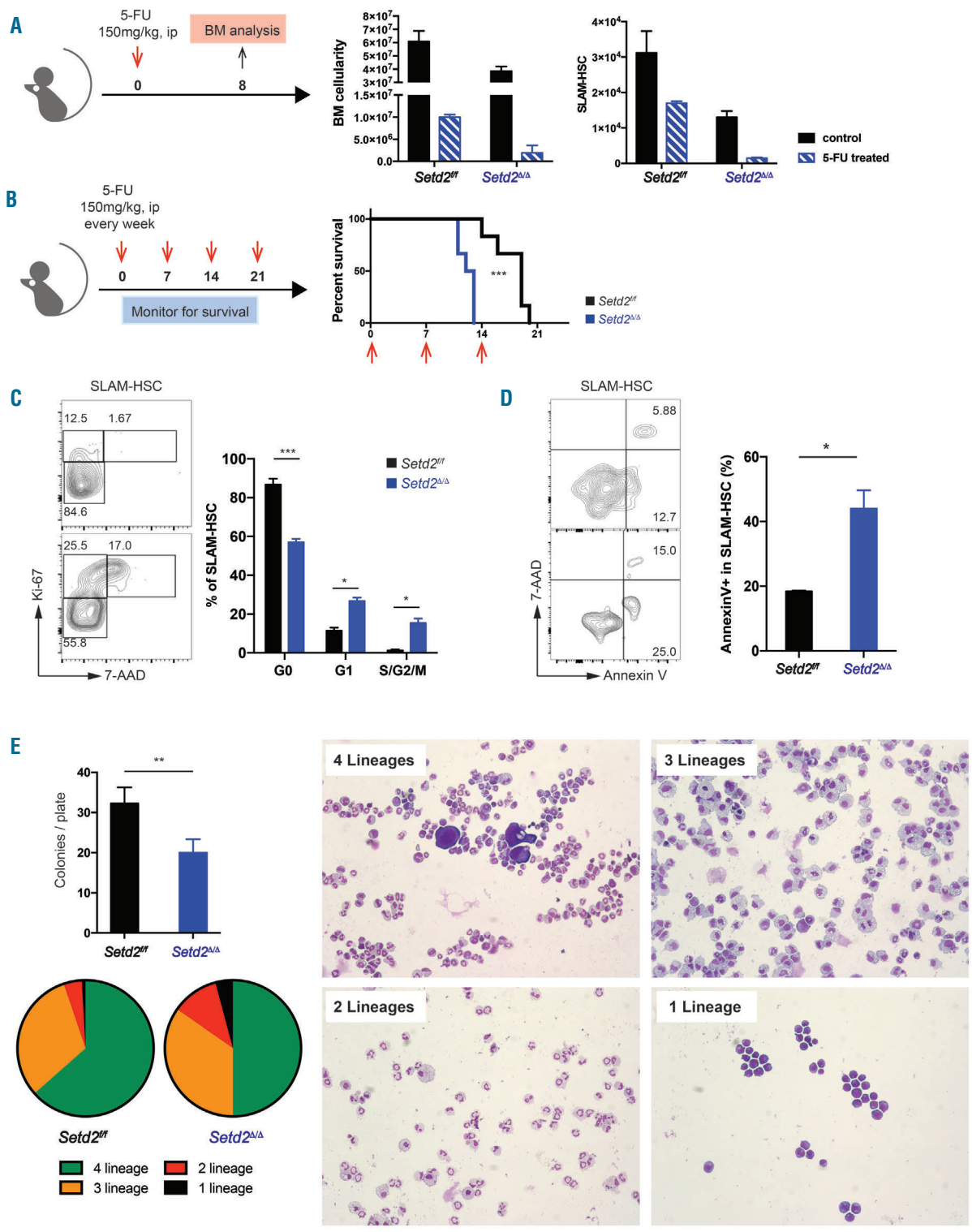

Figure 4. *Setd2*$^{\Delta/\Delta}$ hematopoietic stem cells (HSCs) show reduced quiescence, but increased apoptosis and differentiation. (A) Experimental strategy: *Setd2*$^{f/f}$ and *Setd2*$^{f/f}$*/Vav1-Cre* mice were injected with 150 mg/kg 5-fluorouracil (FU) and sacrificed eight days later (left). Statistical analyses of the bone marrow (BM) cellularity and absolute number of long-term (LT)-HSCs analyzed by flow cytometry (right). Representative data were from 3 independent experiments. (N=6 each genotype; mean±Standard Error of Mean (SEM)]. (B) Experimental strategy: *Setd2*$^{f/f}$ and *Setd2*$^{f/f}$*/Vav1-Cre* mice were injected with 150 mg/kg 5-FU weekly and monitored for survival (left). Survical curve (right) (n=6 each genotype). (C) Flow cytometry analysis of *Setd2*$^{f/f}$ and *Setd2*$^{f/f}$*/Vav1-Cre* BM cells with Ki-67 and 7-AAD. Gating strategy is shown in one representative FACS blots per genotype (left). Summary of statistical analyses showed decreased G0 distribution in *Setd2*$^{f/f}$*/Vav1-Cre* LT-HSCs (right). Representative data were from 3 independent experiments. (N=6 each genotype; mean±SEM). (D) Flow cytometry analysis of *Setd2*$^{f/f}$ and *Setd2*$^{f/f}$*/Vav1-Cre* BM cells with Annexin V and 7-AAD. Gating strategy is shown in one representative FACS blots per genotype (left). Summary of statistical analyses showed increased distribution into AnnexinV positive fraction in *Setd2*$^{f/f}$*/Vav1-Cre* SLAM-HSCs. Representative data were from 3 independent experiments. (N=6 each genotype; mean ± SEM). (E) The bar figure shows the number of clones generated by *Setd2*$^{f/f}$ and *Setd2*$^{f/f}$*/Vav1-Cre* single LT-HSCs per 60-well plate (top left). Pie chart shows the relative frequencies of 4-lineage, 3-lineage, 2-lineage, and 1-lineage clones generated from *Setd2*$^{f/f}$ and *Setd2*$^{f/f}$*/Vav1-Cre* single LT-HSCs (bottom left). Wright's stained cytospin showed representative pictures of 4-lineage, 3-lineage, 2-lineage, and 1-lineage clones generated from *Setd2*$^{f/f}$ and *Setd2*$^{f/f}$*/Vav1-Cre* single LT-HSCs (right). Representative data were from 2 independent experiments. (N=4 each genotype; mean±SEM).

tion of SLAM-HSC is the sole reason to explain the complete loss of HSC functions. We used CD150 and CD48 to define SLAM-HSC, which remains heterogeneous, as reported in recent studies.[20-22] We further analyzed quiescent long-term HSCs with additional defined surface markers besides CD48 and CD150: CD135, CD34, CD201, and CD49b. The results showed that there was a dramatic reduction of $CD201^+CD49b^-$ fraction and a significantly increased entry of $CD201^-CD49b^-$ fraction in the $CD48^-CD150^+CD135^-CD34^-$LSK populations in $Setd2^{\Delta/\Delta}$ mice compared with the control (Figure 5A). It has been reported that $CD201^+$ is an accurate marker in SLAM-HSCs to define the quiescent stem cell pool which is capable of repopulation in bone marrow transplantation,[23,24] and $CD201^+CD49b^-CD135^-CD34^-$ SLAM-HSC population is reputed, as the "true HSC", to have the longest-term self-renewal capacity in deep quiescence.[25] Our data indicate that the real quiescent fractions are further reduced in the decreased SLAM-HSC population in $Setd2^{\Delta/\Delta}$ mice.

To explore the molecular mechanisms underlying HSC regulation by *Setd2*, we performed RNA-seq using LSKs from $Setd2^{f/f}$ and $Setd2^{\Delta/\Delta}$ mice. Unbiased Gene Set Enrichment Analysis (GSEA) revealed that the HSC, long-term HSC, and short-term HSC signature genes[26] were all significantly down-regulated, while intermediate and late progenitor signature genes[26] were significantly up-regulated in $Setd2^{\Delta/\Delta}$ LSKs (Figure 5B), implying that immune-phenotypically defined $Setd2^{\Delta/\Delta}$ HSCs lost the stem cell identity and differentiated toward multipotent progenitors (MPP). Gene ontology analysis of top differentially expressed genes indicated that lineage development/differentiation-related genes were significantly up-regulated in $Setd2^{\Delta/\Delta}$ LSKs (Figure 5C and D, and *Online Supplementary Table S3*), including *Gata1*, *Gata3*, and *Klf1*, which are important in HSC differentiation toward myeloid and lymphoid lineages.

Collectively, loss of Setd2 could induce LT-HSCs to exit from quiescence and commit to differentiation, leading to the exhaustion of LT-HSCs, IT-HSCs, MPP1, and the differentiation to the MPP2, MPP3, and MPP4 populations (Figure 5E).

$Setd2^{\Delta/\Delta}$ HSPCs show increased Nsds and RNA Pol II elongation associated phosphorylation changes

To understand whether loss of Setd2 and H3K36me3 would affect other H3K36-methyltransferases and subsequent methylation states of H3K36, the expression levels of 4 other most closely related enzymes were assessed using LSK cells from BM. Our data showed that Ash1l was decreased, but Nsd1/2/3 were all significantly increased at both mRNA and protein levels (Figure 6A and *Online Supplementary Figure S5A*). Interestingly, when we overexpressed WT *NSD2*, or gain-of-function (GOF) mutant of *NSD2* (*E1099K*) in a murine Mll-Af9 leukemia cell line, both WT *NSD2* and the GOF of *NSD2-E1099K* showed similar H3K36me3/2 changes to LOF of Setd2 (*Online Supplementary Figure S5B*), which implies that Setd2 and Nsds actually antagonize each other's function. LOF SETD2 and GOF NSD2 in human leukemia may result in similar transcriptional dysregulation. Indeed, we found that H3K36me1 and H3K36me2 were dramatically increased, correlated with the up-regulated Nsd1/2/3 (Figure 6B). In addition, H3K4me3 and H3K79me2 were also significantly increased, while H3K27me3 was slightly decreased (Figure 6B), which indicated the promoting transcriptional elongation of RNA polymerase II. The significant increase in elongation-associated phosphorylation changes [RNA pol II (Ser5P) and pol II (Ser2P)] were further confirmed by immunoblotting (Figure 6C). Thus, we hypothesized that *Setd2* knockout up-regulates the RNA pol II transcriptional elongation to activate a subset of genes, which could affect the identity and functions of HSCs.

Our bulk RNA-seq was performed with LSK cells due to limited cell numbers. Next we aimed to define a subset of genes that were up-regulated in $Setd2^{\Delta/\Delta}$ SLAM-HSCs. To identify some candidate genes, the expression profiles of *Setd2* and transcriptional elongation related genes and complexes were checked using a published database.[27] The results showed that BET family genes and some well-known super elongation regulating genes (*Myc*, *Mycn*, *Myb* etc.) were significantly up-regulated during HSC differentiation (*Online Supplementary Figure S6*). Thus, we performed RT-PCR on these up-regulated genes with sorted $Setd2^{\Delta/\Delta}$ SLAM-HSCs. The results showed the dramatic upregulation of *Gata1*, *Gata3*, and *Klf1*, which was consistent with our RNA-seq data (Figure 6D). At the same time, we noticed that Myc was also significantly up-regulated in $Setd2^{\Delta/\Delta}$ SLAM-HSCs (Figure 6D). Myc is well known to be very sensitive to RNA pol II promoter-proximal pausing and releasing from pausing by elongation changes. Importantly, the phenotypes of $Setd2^{\Delta/\Delta}$ HSCs recapitulated the Myc overexpression situation. It has been reported that enforced expression of Myc in SLAM-HSCs promotes differentiation at the expense of self-renewal, inducing exit from quiescence, increased apoptosis, and failure to reconstitute BM in BMT assay,[28] which phenocopies $Setd2^{\Delta/\Delta}$ HSCs. Also, we confirmed the dramatic upregulation of Gata1, Gata3, Klf1, and Myc at the protein level (Figure 6C).

As *Myc* is a well-studied gene, which regulates the entry and exit from stem cell quiescence during development, we first confirmed that the significant increase of Myc is due to enhanced RNA pol II elongation. ChIP-qPCR assays of Setd2, H3K36-related histone modifications, and Pol II were performed at the *Myc* locus using $c\text{-}kit^+$ cells from $Setd2^{f/f}$ and $Setd2^{\Delta/\Delta}$ mice. The results showed that there was a significantly higher enrichment of pol II (Ser5P) and Pol II (Ser2P) occupancy along the whole gene body, promoter and enhancer regions of *Myc* in $Setd2^{\Delta/\Delta}$ HSPCs compared with control.[29,30] Meanwhile, H3K36me2 occupancy also showed a significantly higher enrichment along the gene body, both promoter and enhancers, while the H3K36me1 mainly increased along the enhancer region. As expected, enrichment of Setd2 and H3K36me3 was dramatically reduced, especially at the gene body region (Figure 6E).

$Setd2^{\Delta/\Delta}$ deficiencies could be partially rescued by super elongation complex-related inhibitors

Next, we tested whether the increased gene expressions, such as Myc, could be reversed by epigenetic drugs. The $c\text{-}kit^+$ $Setd2^{\Delta/\Delta}$ cells were treated in an *in vitro* culture assay with super elongation complex (SEC) related inhibitors for 24 and 48 h: JQ1 (Brd4 inhibitor), EPZ-5676 (Dot1l inhibitor), and BAY 1143572 (p-TEFb/CDK9 inhibitor). The elevated H3K36me1/2 marks were not affected 48 h after treatment (Figure 7A), while the expression levels of pol II (Ser2P), pol II (Ser5P), Gata1, Gata3, and Myc were significantly decreased in all 3 drug-treated

groups (Figure 7B). This indicated that Nsds-mediated H3K36me1/2 modifications were upstream of SEC complex recruitment and releasing promoter-proximal pausing of pol II. Meanwhile, SEC complex inhibitors could not affect other genes such as Gapdh and β-actin (Figure 7B).

Besides the changes of protein expression levels, the functional changes were also assessed. The c-kit^{+} *Setd2*$^{\Delta/\Delta}$ cells were treated *in vitro* for 24 h with 3 inhibitors respectively, and LSK populations were further gated to analyze the apoptotic and cell cycle status. There were significant-

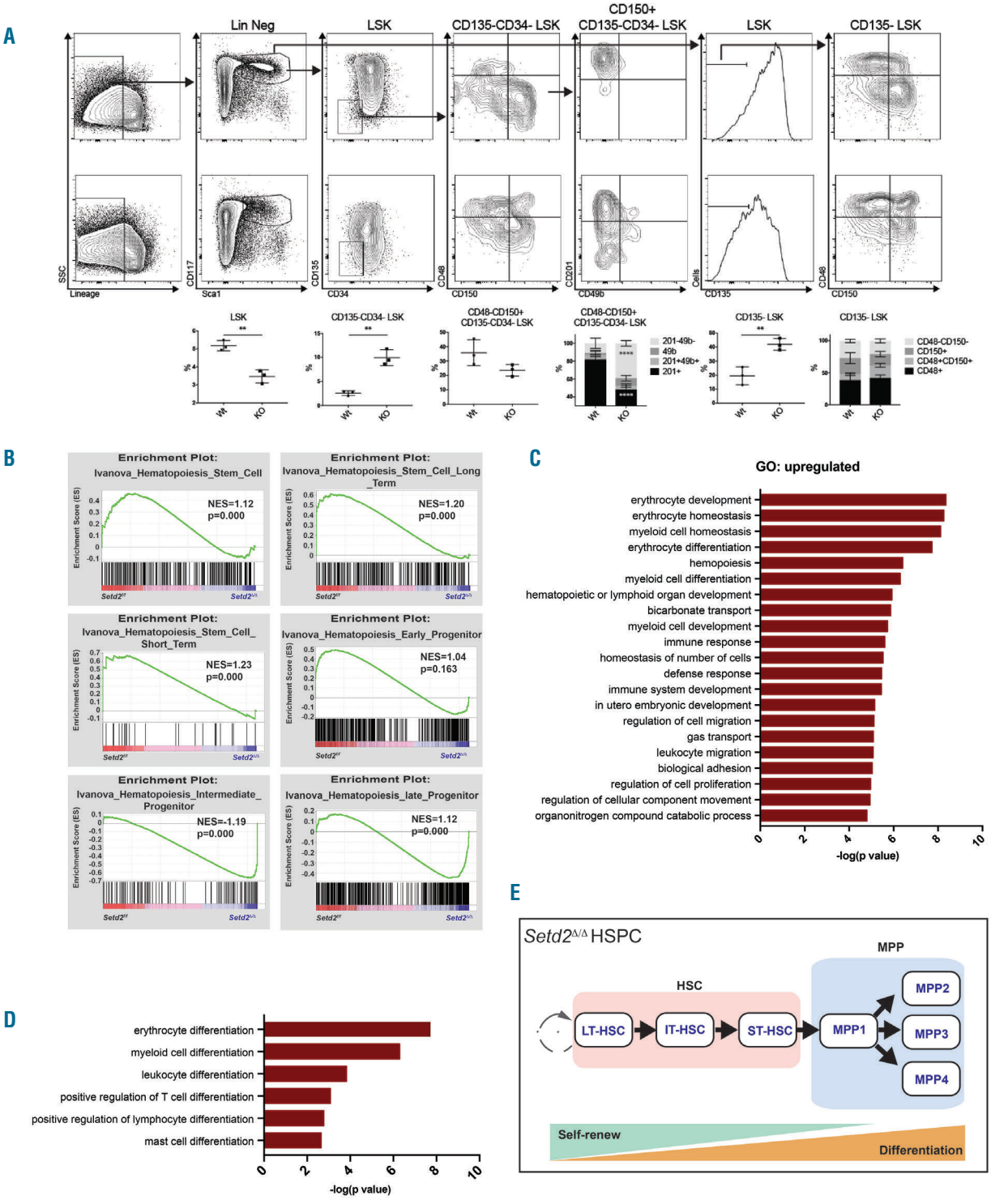

Figure 5. *Setd2*$^{\Delta/\Delta}$ hematopoietic stem cells (HSCs) show loss of stem cell identity and increased differentiation toward progenitors. (A) Flow cytometry analysis of *Setd2*$^{f/f}$ and *Setd2*$^{f/f}$*/Vav1-Cre* mice bone marrow (BM) cells. [N=3 each genotype; mean±Standard Error of Mean (SEM)]. (B) Gene Set Enrichment Analysis (GSEA) for genes affected in the LSKs of *Setd2*$^{f/f}$ and *Setd2*$^{f/f}$*/Vav1-Cre* mice, after RNA-seq analyses. (A-E) Enrichment of HSC, long-term (LT)-HSC, short-term (ST)-HSC, early progenitors, intermediate progenitors, and late progenitors gene sets in LSKs of *Setd2*$^{f/f}$ and *Setd2*$^{f/f}$*/Vav1-Cre* mice, respectively. All gene sets are from GSEA molecular signature database.[26] (C and D) Up-regulated gene ontology analysis of differentially expressed genes. (E) Diagram of *Setd2*$^{\Delta/\Delta}$ HSPC differentiation.

ly decreased Annexin V$^+$ fractions and increased G0 fractions in all 3 drug-treated groups compared with PBS treated group (Figure 7C-F), which indicates that SEC complex inhibitors could partially rescue the HSC functional deficiencies in *Setd2*$^{\Delta/\Delta}$ cells. However, the *in vitro* single-cell differentiation assays failed due to the toxicity of those inhibitors in a long-term treatment.

Collectively, based on our results and published data, we propose a model for Setd2 function in HSCs (Figure 8). Setd2 loss leads to the significant upregulation of Nsds,

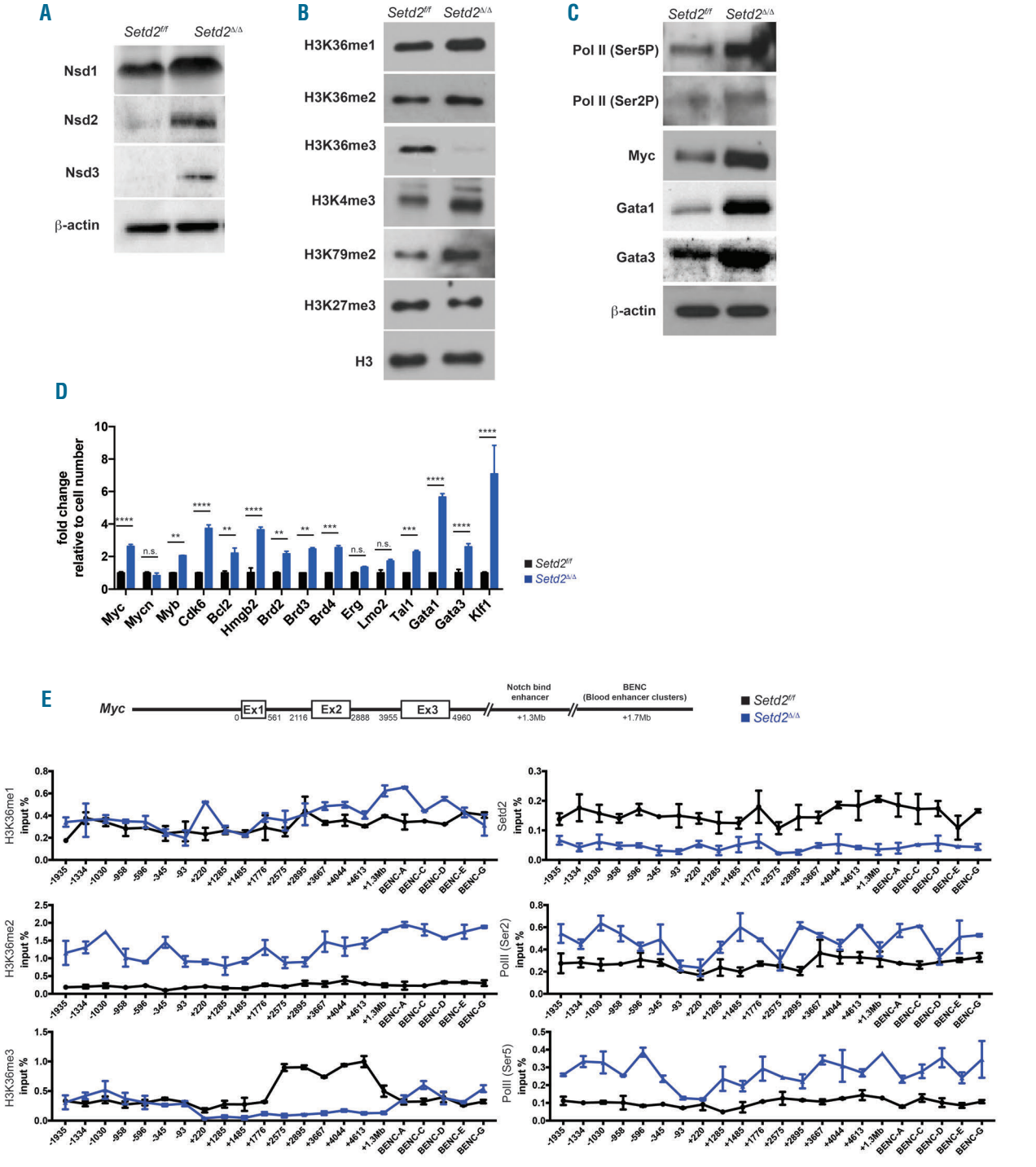

Figure 6. *Setd2*$^{\Delta/\Delta}$ hematopoietic stem cells (HSCs) show increased Nsds and RNA Pol II elongation associated phosphorylation changes. (A) Nsd1/2/3 and β-actin levels were determined by immunoblotting using bone marrow (BM) LSK cells. (B and C) H3K36me1/2, H3K4me3, H3K79me2, H3K27me3, H3, RNA pol II (Ser2P), pol II (Ser5P), Gata1, Gata3, Klf1, Myc, and β-actin levels were determined by immunoblotting using BM LSK cells from *Setd2*$^{f/f}$ and *Setd2*$^{f/f}$*/Vav1-Cre* mice. (D) Relative gene expression levels were determined by qrt-PCR using flow sorted SLAM-HSCs from *Setd2*$^{f/f}$ and *Setd2*$^{f/f}$*/Vav1-Cre* mice. Representative data were from 3 independent experiments. [N=6 each genotype; mean±Standard Error of Mean (SEM)]. (E) ChIP-qPCR assays of Setd2, Setd2 related histone modifications, and pol II phosphorylated forms [Pol II (Ser5P) and pol II (Ser2P)] on Myc locus was determined with c-kit$^+$ BM cells from *Setd2*$^{f/f}$ and *Setd2*$^{f/f}$*/Vav1-Cre* mice. (*Setd2*$^{f/f}$=5 and *Setd2*$^{f/f}$*/Vav1-Cre*=8; mean±SEM from 2 independent experiments).

which could recruit Brd4,[31-34] whereas Brd4 could recruit DOT1L complex and p-TEFb complex to increase p-TEFb-dependent phosphorylation of pol II CTD and stimulate transcription from promoters that have promoter-proximal pausing.[35-37] Such enhanced pol II elongation could result in the upregulation of a subset of genes including *Myc*, which controls the balance of quiescence and differentiation in HSCs.

Discussion

In this study, we generated a novel conditional knockout allele (*Setd2*$^{\Delta/\Delta}$). These mice manifested leukopenia, macrocytic anemia, increased platelet, and erythroid dysplasia in BM, which are comparable to the phenotypes of myelodysplastic syndromes (MDS) associated with isolated del(5q). It has been reported that rare *SETD2* mutations

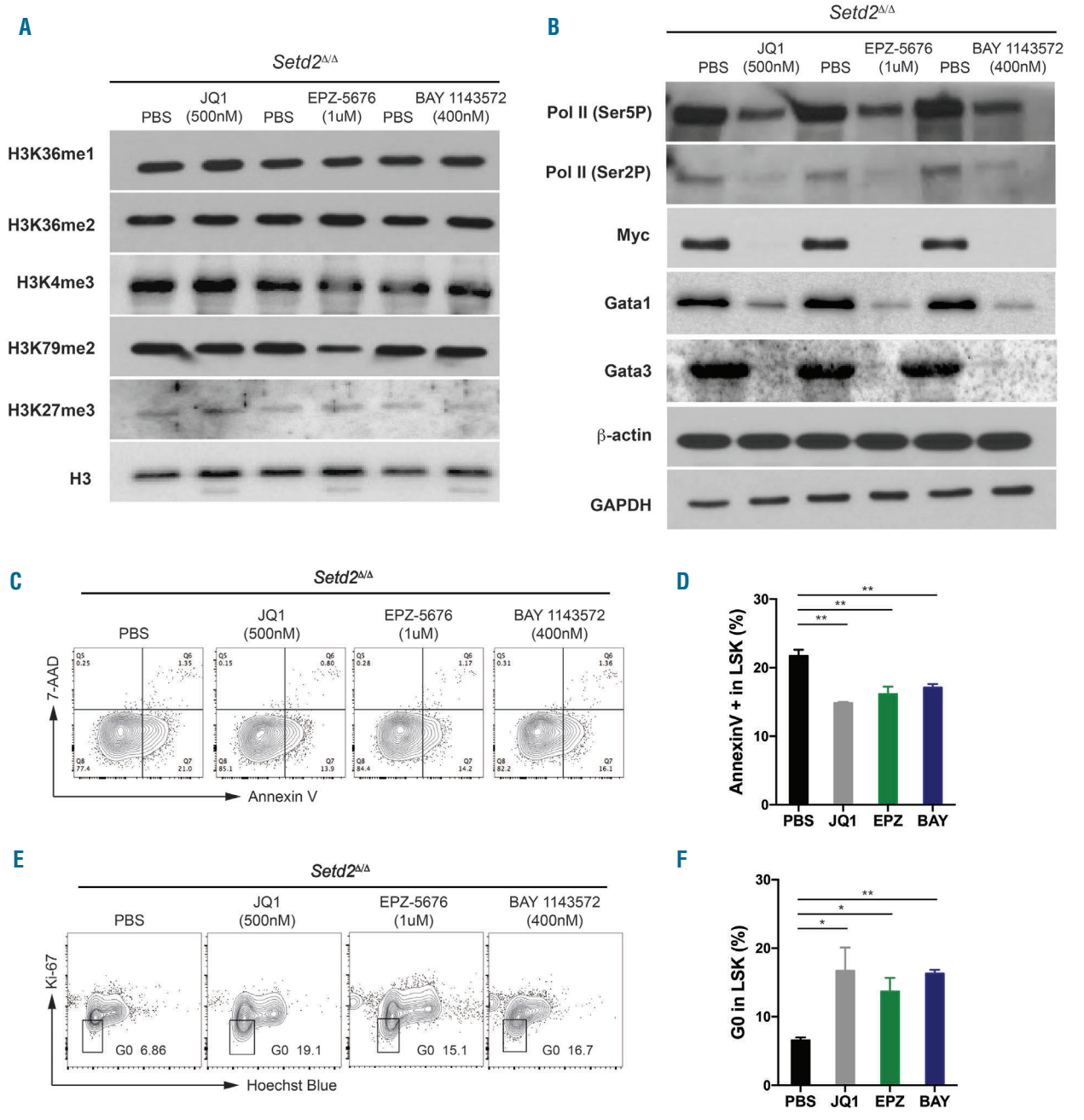

Figure 7. *Setd2*$^{\Delta/\Delta}$ deficiencies could be partially rescued by super elongation complex-related inhibitors. (A and B) Treatment of c-Kit$^+$ bone marrow (BM) cells from *Setd2*$^{f/f}$*/Vav1-Cre* mice with JQ1 500nM, EPZ-5676 1uM, BAY 1143572 400 nM for 24 h (h). Then cells were collected to determine the proteins levels of H3K36me1/2, H3K4me3, H3K79me2, H3K27me3, H3, RNA pol II (Ser2P), pol II (Ser5P), Gata1, Gata3, Myc, and β-actin by immunoblotting. (C and D) Flow cytometry analysis of drug-treated c-kit$^+$ cells from *Setd2*$^{f/f}$ and *Setd2*$^{f/f}$*/Vav1-Cre* mice with Annexin V and 7-AAD. Gating strategy is shown in one representative FACS blot per genotype. Summary of statistical analyses showed decreased distribution into AnnexinV positive fraction in drug-treated groups. Representative data were from 3 independent experiments. (*Setd2*$^{f/f}$*=6* and *Setd2*$^{f/f}$*/Vav1-Cre=12*). (E and F) Flow cytometry analysis of drug treated c-kit$^+$ cells from *Setd2*$^{f/f}$ and *Setd2*$^{f/f}$*/Vav1-Cre* mice with Ki67 and Hoechst blue. Gating strategy is shown in one representative FACS blot per genotype. Summary of statistical analyses showed increased distribution into G0 fraction in drug-treated groups. Representative data are from 3 independent experiments; (*Setd2*$^{f/f}$*=6* and *Setd2*$^{f/f}$*/Vav1-Cre=12*).

were identified in MDS patients,[38] but whether *SETD2* is involved in MDS development is still unclear. To examine whether *SETD2* is down-regulated in MDS del(5q), we checked *SETD2* expression levels in an MDS del(5q) cohort with 3 different probes. However, no significant differences between del(5q) and the control groups were found (*Online Supplementary Figure S5A*). Besides erythroid dysplasia and BM fibrosis,[39] there are increased proportions of erythroblasts in the BM. Moreover, as the *Setd2*$^{\Delta/\Delta}$ mice became older, the percentage of erythroblasts accumulated and could even reach up to 80% in some mice, which is somewhat similar to the BM of acute erythroid leukemia (pure erythroid type).[40]

It is clear that Setd2 plays a critical role in maintaining the identity and functions of HSCs. *Setd2*$^{\Delta/\Delta}$ mice showed reduced HSCs and capability of BM reconstitution after transplantation. *Setd2*$^{\Delta/\Delta}$ HSCs showed loss of quiescence, increased apoptosis, and reduced multi-potent differentiation potential. Unbiased GSEA and GO analysis also indicated the upregulation of lineage development/differentiation pathways and related genes. Thus, there could be two explanations for the dramatic reduction in HSC numbers. First, some HSCs exited from quiescence and committed to differentiation. The balance between self-renewal and differentiation is important for the maintenance of the stem cell pool. Pushing HSCs to differentiate would come at the expense of self-renewal and lead to the exhaustion of HSCs. The other reason could be that some HSCs directly underwent cell death. However, *Setd2*$^{\Delta/\Delta}$ mice did not progress to pancytopenia and BM failure without a stress challenge; this is in line with the finding that, at steady stage, a limited number of HSPCs would be sufficient to maintain normal hematopoiesis.[41]

Setd2, a histone methyltransferse, regulates H3K36me3. The direct effect after Setd2 knockout is the impact on histone modifications and other closely related H3K36 methyltransferases. Thus, the expression levels of Ash1l, Nsd1/2/3, and related histone markers were assessed first. The results showed significantly up-regulated Nsd1/2/3, accompanied with increased H3K36me1 and H3K36me2. Recently, we found that downregulation of SETD2 leads to a global elevation of DOT1L-mediated H3K79me2 in MLL-AF9 leukemia.[42] Consistent with this finding, we observed a dramatic increase in H3K79me2 and H3K4me3, implying the promoting of transcriptional elongation. The enhanced RNA pol II elongation was further confirmed by the up-regulated pol II (Ser2P) and pol II (Ser5P) phosphorylations. We confirmed the significant upregulation of Gata1, Gata3, Klf1, and Myc in *Setd2*$^{\Delta/\Delta}$ SLAM-HSCs. These subsets of genes are sensitive to enhanced pol II elongation.

The enhanced elongation after Setd2 knockout was

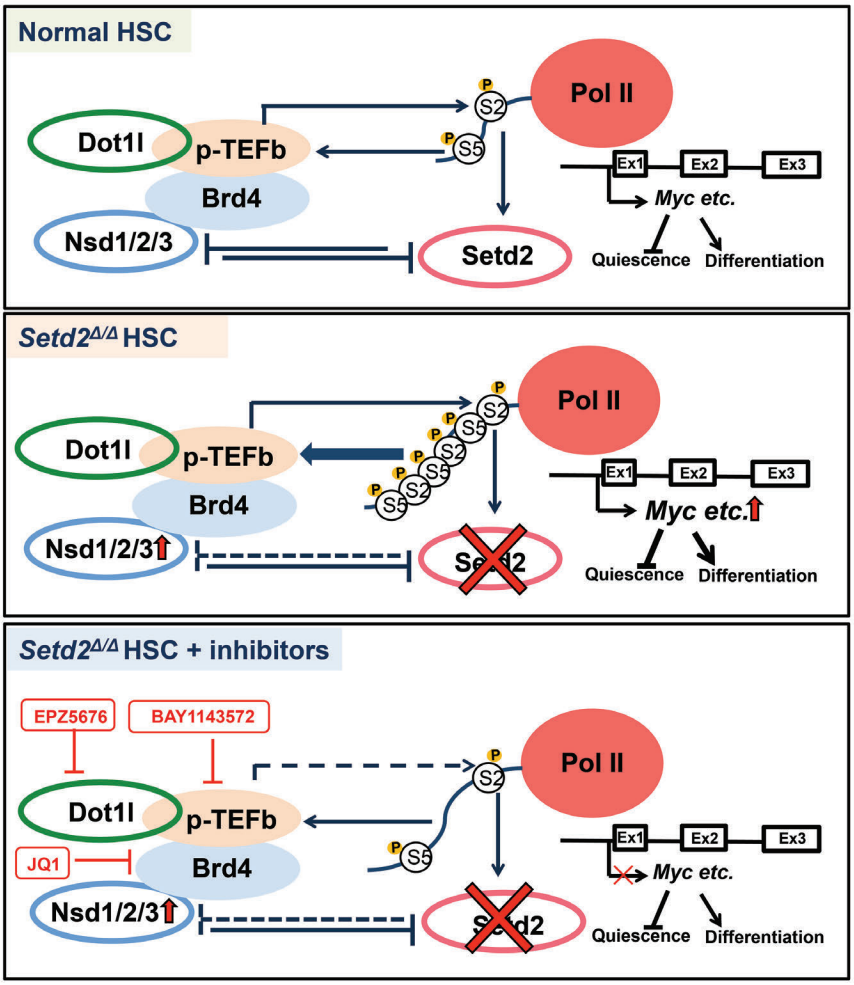

Figure 8. The diagram of our working model. In normal adult hematopoietic stem cells (HSCs), Setd2, responsible for H3K36me3, could repress Nsds, which are responsible for H3K36me1/2. Nsds interact with Brd4, p-TEFb, and Dot1l to stimulate transcriptional elongation. On the other hand, Setd2 binds to pol II (Ser2P) and pol II (Ser5P) doubly modified CTD repeats. Thus, a subset of genes, such as *Myc*, is maintained at a proper level to keep the balance between quiescence and differentiation of adult stem cells (top). In *Setd2*$^{\Delta/\Delta}$ HSCs, *Setd2* loss leads to the upregulation of NSDs, which would further enhance the Pol II phosphorylation and elongation, resulting in the upregulation of *Myc*. When treated with Brd4/Dot1l/p-TEFb inhibitors, the pol II (Ser2), pol II (Ser5), and the expressions of the *Myc* could be down-regulated (bottom).

clearly indicated by globally elevated marks. The higher enrichment of pol II (Ser5P) and pol II (Ser2P) occupancy were also confirmed on *Myc* locus in *Setd2*$^{\Delta/\Delta}$ HSPCs. Setd2 and H3K36me3 generally mark the active genes; however, our surprising findings indicated that Setd2-H3K36me3 restrict the pol II elongation. To connect the Setd2 loss to enhanced elongation, we observed upregulations of Nsd1/2/3 after Setd2 knockout. There is much literature showing that NSDs could interact with BRD4, which could bridge to the SEC and DOT1l complex.[31-34] Thus, we proposed a regulatory model in which there is a crosstalk between Setd2 and Nsds. Loss of Setd2 leads to the upregulation of Nsds. Meanwhile, Nsds could interact with Brd4, SEC, and Dot1l complex to enhance the elongation, and results in the upregulation of a subset of target genes that regulate quiescence and differentiation of HSCs.

In summary, using our novel Setd2 conditional knockout allele, we revealed unique roles of *Setd2* in regulating quiescence and differentiation of HSCs. Our study not only provides us with a deeper understanding of Setd2 functions in HSCs, but also a better understanding of SETD2 functions during leukemic transformation and solid tumors. Along with using the KDM4 inhibitor to restore the H3K36me3,[43] inhibiting the elongation complex or downstream targets, could be effective for LOF mutation *SETD2* in cancer and could also benefit bi-allele *SETD2* mutant patients. Our data also indicate that GOF mutation of NSDs, such as NSD2 mutations or NSD1/3 translocations, might follow the same regulatory dysregulation as LOF of SETD2 on pol II elongation in leukemia and other cancers.

Acknowledgments

We would like to thank Cincinnati Children's Research Flow Cytometry Core (RFCC), Cincinnati Children's Veterinary Services, and CCHMC mouse core. We would also like to thank Damien Reynaud and George Mike Freudiger for their help on this project. This work was supported by grants from the Ministry of Science and Technology of China (2016YFA0100600) (to TC), the National Natural Science Foundation of China (81421002) (to TC), CAMS Initiative for Innovative Medicine (2016-I2M-1-017) (to TC), Leukemia Research Innovative Team of Zhejiang Province (2011R50015) (to JJ), National Natural Science Foundation of China (81370643-H0812) (to JJ), the CFK (to GH), National Institutes of Health (NIH) (R21CA187276) (to GH).

References

1. Kiel MJ, Yilmaz OH, Iwashita T, et al. SLAM family receptors distinguish hematopoietic stem and progenitor cells and reveal endothelial niches for stem cells. Cell. 2005;121(7):1109-1121.
2. Orkin SH, Zon LI. Hematopoiesis: an evolving paradigm for stem cell biology. Cell. 2008;132(4):631-644.
3. Dawson MA, Kouzarides T. Cancer epigenetics: from mechanism to therapy. Cell. 2012;150(1):12-27.
4. Oike T, Ogiwara H, Amornwichet N, Nakano T, Kohno T. Chromatin-regulating proteins as targets for cancer therapy. J Radiat Res. 2014;55(4):613-628.
5. Strahl BD, Grant PA, Briggs SD, et al. Set2 is a nucleosomal histone H3-selective methyltransferase that mediates transcriptional repression. Mol Cell Biol. 2002;22(5):1298-1306.
6. McDaniel SL, Strahl BD. Shaping the cellular landscape with Set2/SETD2 methylation. Cell Mol Life Sci. 2017;74(18):3317-3334.
7. Mao M, Fu G, Wu JS, et al. Identification of genes expressed in human CD34(+) hematopoietic stem/progenitor cells by expressed sequence tags and efficient full-length cDNA cloning. Proc Natl Acad Sci USA. 1998;95(14):8175-8180.
8. Wagner EJ, Carpenter PB. Understanding the language of Lys36 methylation at histone H3. Nat Rev Mol Cell Biol. 2012;13(2):115-126.
9. Vougiouklakis T, Hamamoto R, Nakamura Y, Saloura V. The NSD family of protein methyltransferases in human cancer. Epigenomics. 2015;7(5):863-874.
10. Zhang Y, Xie S, Zhou Y, et al. H3K36 histone methyltransferase Setd2 is required for murine embryonic stem cell differentiation toward endoderm. Cell Rep. 2014;8(6):1989-2002.
11. Hu M, Sun XJ, Zhang YL, et al. Histone H3 lysine 36 methyltransferase Hypb/Setd2 is required for embryonic vascular remodeling. Proc Natl Sci USA. 2010;107(7):2956-2961.
12. Fahey CC, Davis IJ. SETting the Stage for Cancer Development: SETD2 and the Consequences of Lost Methylation. Cold Spring Harb Perspect Med. 2017;7(5).
13. Zhang J, Ding L, Holmfeldt L, et al. The genetic basis of early T-cell precursor acute lymphoblastic leukaemia. Nature. 2012;481(7380):157-163.
14. Parker H, Rose-Zerilli MJ, Larrayoz M, et al. Genomic disruption of the histone methyltransferase SETD2 in chronic lymphocytic leukaemia. Leukemia. 2016;30(11):2179-2186.
15. Moffitt AB, Ondrejka SL, McKinney M, et al. Enteropathy-associated T cell lymphoma subtypes are characterized by loss of function of SETD2. J Exp Med. 2017;214(5):1371-1386.
16. Zhu X, He F, Zeng H, et al. Identification of functional cooperative mutations of SETD2 in human acute leukemia. Nat Genet. 2014;46(3):287-293.
17. Speck NA, Iruela-Arispe ML. Conditional Cre/LoxP strategies for the study of hematopoietic stem cell formation. Blood Cells Mol Dis. 2009;43(1):6-11.
18. Kvasnicka HM, Beham-Schmid C, Bob R, et al. Problems and pitfalls in grading of bone marrow fibrosis, collagen deposition and osteosclerosis - a consensus-based study. Histopathology. 2016;68(6):905-915.
19. Cheng T, Rodrigues N, Shen H, et al. Hematopoietic stem cell quiescence maintained by p21cip1/waf1. Science. 2000;287(5459):1804-1808.
20. Oguro H, Ding L, Morrison SJ. SLAM family markers resolve functionally distinct subpopulations of hematopoietic stem cells and multipotent progenitors. Cell Stem Cell. 2013;13(1):102-116.
21. Raaijmakers MH, Scadden DT. Divided within: heterogeneity within adult stem cell pools. Cell. 2008;135(6):1006-1008.
22. Wilson A, Laurenti E, Oser G, et al. Hematopoietic stem cells reversibly switch from dormancy to self-renewal during homeostasis and repair. Cell. 2008;135(6):1118-1129.
23. Balazs AB, Fabian AJ, Esmon CT, Mulligan RC. Endothelial protein C receptor (CD201) explicitly identifies hematopoietic stem cells in murine bone marrow. Blood. 2006;107(6):2317-2321.
24. Kent DG, Copley MR, Benz C, et al. Prospective isolation and molecular characterization of hematopoietic stem cells with durable self-renewal potential. Blood. 2009;113(25):6342-6350.
25. Schroeder T. Hematopoietic stem cell heterogeneity: subtypes, not unpredictable behavior. Cell Stem Cell. 2010;6(3):203-207.
26. Ivanova NB, Dimos JT, Schaniel C, et al. A stem cell molecular signature. Science. 2002;298(5593):601-604.
27. Cabezas-Wallscheid N, Buettner F, Sommerkamp P, et al. Vitamin A-Retinoic Acid Signaling Regulates Hematopoietic Stem Cell Dormancy. Cell. 2017;169(5):807-823 e819.
28. Wilson A, Murphy MJ, Oskarsson T, et al. c-Myc controls the balance between hematopoietic stem cell self-renewal and differentiation. Genes Dev. 2004;18(22):2747-2763.
29. Herranz D, Ambesi-Impiombato A, Palomero T, et al. A NOTCH1-driven MYC enhancer promotes T cell development, transformation and acute lymphoblastic leukemia. Nat Med. 2014;20(10):1130-1137.
30. Bahr C, von Paleske L, Uslu VV, et al. A Myc enhancer cluster regulates normal and leukaemic haematopoietic stem cell hierarchies. Nature. 2018;553(7689):515-520.
31. Zhang Q, Zeng L, Shen C, et al. Structural Mechanism of Transcriptional Regulator NSD3 Recognition by the ET Domain of BRD4. Structure. 2016;24(7):1201-1208.
32. Sarai N, Nimura K, Tamura T, et al. WHSC1 links transcription elongation to HIRA-

mediated histone H3.3 deposition. EMBO J. 2013;32(17):2392-2406.
33. Shen C, Ipsaro JJ, Shi J, et al. NSD3-Short Is an Adaptor Protein that Couples BRD4 to the CHD8 Chromatin Remodeler. Mol Cell. 2015;60(6):847-859.
34. Rahman S, Sowa ME, Ottinger M, et al. The Brd4 extraterminal domain confers transcription activation independent of pTEFb by recruiting multiple proteins, including NSD3. Mol Cell Biol. 2011;31(13):2641-2652.
35. Jang MK, Mochizuki K, Zhou M, et al. The bromodomain protein Brd4 is a positive regulatory component of P-TEFb and stimulates RNA polymerase II-dependent transcription. Mol Cell. 2005;19(4):523-534.
36. Yang Z, Yik JH, Chen R, et al. Recruitment of P-TEFb for stimulation of transcriptional elongation by the bromodomain protein Brd4. Mol Cell. 2005;19(4):535-545.
37. Benedikt A, Baltruschat S, Scholz B, et al. The leukemogenic AF4-MLL fusion protein causes P-TEFb kinase activation and altered epigenetic signatures. Leukemia. 2011;25(1):135-144.
38. Haferlach T, Nagata Y, Grossmann V, et al. Landscape of genetic lesions in 944 patients with myelodysplastic syndromes. Leukemia. 2014;28(2):241-247.
39. Della Porta MG, Malcovati L. Myelodysplastic syndromes with bone marrow fibrosis. Haematologica. 2011;96(2):180-183.
40. Arber DA, Orazi A, Hasserjian R, et al. The 2016 revision to the World Health Organization classification of myeloid neoplasms and acute leukemia. Blood. 2016;127(20):2391-2405.
41. Busch K, Klapproth K, Barile M, et al. Fundamental properties of unperturbed haematopoiesis from stem cells in vivo. Nature. 2015;518(7540):542-546.
42. Bu J, Chen A, Yan X, et al. SETD2-mediated crosstalk between H3K36me3 and H3K79me2 in MLL-rearranged leukemia. Leukemia. 2018;32(4):890-899.
43. Mar BG, Chu SH, Kahn JD, et al. SETD2 alterations impair DNA damage recognition and lead to resistance to chemotherapy in leukemia. Blood. 2017;130(24):2631-2641.